

Identification of Fault Structure in the Vicinity of Bukik Gadang Hot Spring Mount Talang Subdistrict Using Geomagnetic Method

Ikhwan Fikri Maulidan¹, Marzuki¹, Ardian Putra^{1*}

¹Department of Physics, Universitas Andalas, Limau Manis, Padang 25163, Indonesia.

Received: August 3, 2022

Revised: October 2, 2022

Accepted: October 15, 2022

Published: October 31, 2022

Corresponding Author:

Ardian Putra

ardianputra@sci.unand.ac.id

© 2022 The Authors. This open access article is distributed under a (CC-BY License)



DOI: [10.29303/jppipa.v8i4.1962](https://doi.org/10.29303/jppipa.v8i4.1962)

Abstract: Geological structures in the Bukit Gadang geothermal area have been identified using the geomagnetic method to determine the type of fault. Data was measured using a magnetometer in the area with dimensions of 1200 m × 1200 m consisting of 144 points at 12 tracks, and the spacing between points was 100 m. Magnetic anomaly data performed diurnal and IGRF (International Geomagnetic Reference Field) corrections. Furthermore, reduced to poles and continuous upwards processes were carried out to remove noise and separate local and regional anomalies. The magnetic field anomaly in the study area ranges from -1771.8 nT to 1089.9 nT, dominated by negative values, indicating the presence of heat sources and the influence of demagnetization of subsurface rocks. The 2D modeling results show that two primary rocks dominate the study area; pyroclastic flow units and andesite lava rock, which come from the Jantan and Batino volcanic formations. The caprock rock layer was identified in the upper layer with a depth of 850 meters. The reservoir rock layer with low susceptibility values was below the caprock layer. The 3D modeling results show a normal fault with a depth of 300-800 meters or at the border of the Jantan volcanic formation with the Batino volcanic formation. The fault line leads to the southeast-northwest (N160°E). The faults obtained from the 2D and 3D models are suspected to be the outflow of geothermal fluid from the reservoir rock layer and form a manifestation in the form of a hot spring at Bukik Gadang.

Keywords: Bukik Gadang; Fault; Geomagnetic; Susceptibility

Introduction

The existence of an active volcanic path in West Sumatera makes this region has a lot of geothermal potential. It is spread over the districts of Pasaman, West Pasaman, Lima Puluh Kota, Tanah Datar, Agam, Solok, and South Solok (Dinas Pertambangan dan Energi Provinsi Sumatera Barat, 2017). This condition is related to the position of West Sumatra which is located at the confluence of two plates, namely Indo-Australian plate and Eurasian plate and there is a Semangko fault (Munandar et al., 2003). The process of plate collisions produces magmatic pathways along the islands and oceans they pass through. Evidence of the collision of the Indo-Australian Plate and the Eurasian Plate can be seen

from a series of active volcanoes, including Mount Talang in Solok (Naryanto, 1997).

Mount Talang geothermal field is typical of a stratovolcanoes (volcanic) geothermal system, located in the northeast of Talang Volcanoes (mainly andesite), and is situated in the middle of Great Sumatra Fault zone (Rohaendi & Agustine, 2016). The area is covered by Pre-Tertiary-Quaternary rocks that composed of metamorphic rocks (Trts: phyllite), old volcanic rocks (QTau: andesite, tuff breccia), lava (QLv: andesite, tuff breccia, pyroclastic) and surface deposit (QLh) (Idral, 2011). The metamorphic and volcanic rocks are mostly weathered, the volcanic rocks are also altered in some places that characterized by sericite and chlorite alteration mineral assemblage (Idral, 2011).

How to Cite:

Marzuki, M., Maulidan, I. F., & Putra, A. (2022). Identification of Fault Structure in the Vicinity of Bukik Gadang Hot Spring Mount Talang Subdistrict Using Geomagnetic Method. *Jurnal Penelitian Pendidikan IPA*, 8(4), 1856-1862. <https://doi.org/10.29303/jppipa.v8i4.1962>

One of the areas in Mount Talang that has geothermal prospects is Nagari Sungai Janiah, Gunung Talang District. This potential is evidenced by the presence of surface manifestations in the form of Bukit Gadang hot springs with a surface temperature of 43.1°C and a pH of 8.2 (Utami & Putra, 2018). In this region, it is also found hot springs, steaming ground, hydrothermal eruption, and alteration rocks, as well as the results of previous investigations showing the existence of a geothermal system in the area (Munandar et al., 2003). The appearance of several surface manifestations around Mount Talang is thought to be closely related to the activity of andesitic magma and subduction areas on the periphery of the active continent between the Indo-Australian plate and the Eurasian plate (Qodri & Putra, 2018).

Hot spring type performed using geochemistry method is classified as a sulfate fluid. Sulfate content is between 80.00 mg/L to 193.75 mg/L, meaning that the hot springs formed by an active volcanic system have moderate depth characteristics (Hidayat & Putra, 2014). Kholid et al., using the magnetotelluric method, found that the geothermal reservoir is estimated to be under the cap rock which is found in the southern part. The peak of this reservoir is at a depth of about 1800 m and deepens towards the north which can reach a depth of about 2500 m (Kholid & Marpaung, 2011). Research related to fluid characteristics and reservoir temperature estimation by Utami and Putra (2018) around Mount Talang shows that the fluid is in immature water indicating that the geothermal reservoir fluid has been diluted with other elements. The reservoir fluid comes from a new hydrothermal system influenced by the magma of Mount Talang. The estimated temperature of the geothermal reservoir using a silica geothermometer is 147 °C - 179 °C, which is included in the medium-temperature geothermal system (Utami & Putra, 2018).

Based on previous studies, it is not clear how surface manifestations such as hot water around Mount Talang can be formed from geothermal fluid flows from the reservoir. Therefore, this research will conduct a geomagnetic survey in the area of the Bukit Gadang hot spring manifestation area to predict how the hot water can form and emerge to the surface. The appearance of the manifestation in the form of hot water is closely related to the presence of fault lines or faults passing through it (Sundhoro et al., 2001). Faults are important for understanding geothermal systems due to their influence on the stratigraphic structure, and how that structure influences fluid flow (Corbel et al., 2012; Siler et al., 2019). These faults will eventually be directly related to the origin of the geothermal fluid (reservoir) as the main source of thermal energy for a geothermal system (Fitrochaton Chasanah et al., 2018). There have been several researchers who have successfully used this method in geothermal and fault cases such as Hanafy

(2012), Mawarni (2018), Maulidan (2021), and Bukhari (2019). This method can be done by measuring the magnetic field on the surface of the geothermal energy area. The existence of geothermal energy generally depends on faults around geothermal sources. Steam and hot water usually release to the surface through cracks or fractures. The Gunung Talang geothermal system can be presumed to be related to faults in the geothermal source area. Therefore, it is necessary to study the existence and model of faults in this geothermal system area. The geomagnetic method is one of the simplest geophysical methods in the data collection process compared to other methods (Heningtyas et al., 2020). This method measures the total magnetic field of the earth at a place using a magnetometer with high measurement accuracy and can detect deep subsurface (El All et al., 2015).

Method

This research generally consists of literature study and field study, data collection, data processing, 2D and 3D modeling, and data interpretation which can be seen in the following flow chart (Figure 1).

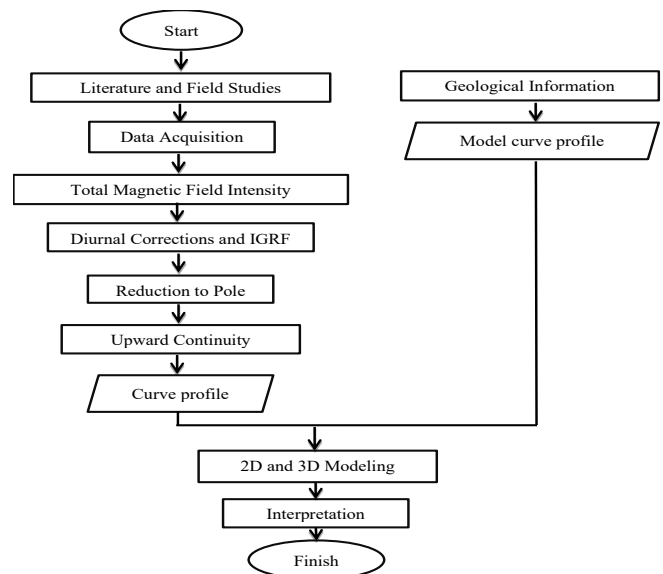


Figure 1. Research Technique Flowchart

Data Acquisition

The location of data collection is in Nagari Sungai Janiah, Gunung Talang District, Solok Regency. Data acquisition was carried out by measuring the value of the total magnetic field in the research area. Field measurement data was performed using a closed-loop method. Magnetic field data retrieval was carried out in an area of 1,243,225 m² around the hot spring which has 12 tracks with a distance of 100 m between tracks and each track has 12 points with a distance of 100 m between points as can be seen in Figure 2.

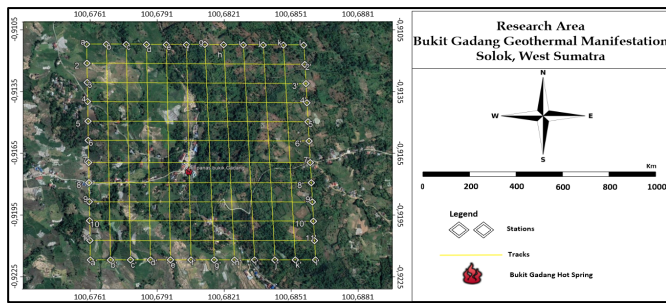


Figure 2. Map of study area

Data Processing

Data processing begins with making a contour map of the total magnetic field induction obtained from the acquisition of magnetic data, then the IGRF (International Geomagnetic Reference Field) and diurnal variation correction was carried out to obtain the total magnetic field anomaly value using Equation (1).

$$\Delta H = H_p - H_{IGRF} \pm H_d \tag{1}$$

where ΔH is the magnetic anomaly, H_p is the measured magnetic field, H_{IGRF} is the theoretical magnetic field of IGRF correction, and H_d is the diurnal correction. The total magnetic anomaly value is interpreted in the contour map, then followed by the transformation of the magnetic field process. The first transformation is reduction to the pole to eliminate the magnetic dipole effect and the inclination effect. The second transformation is an upward continuity to reduce the influence of local magnetic anomalies and emphasize the influence of regional magnetic anomalies on the contour map. The regional magnetic anomaly contour map resulted from the separation of the anomaly is then sliced. The slice results are described by 2D modeling using Oasis Montaj. Final stage is the process of analysis and interpretation of fault models and subsurface rock structures. The model obtained from the modeling results is used in making 3D views using RockWorks 17 software.

Result and Discussion

Magnetic Anomaly

Figure 3 shows the magnetic field anomaly values ranging from -1730.4 nT to 1909.0 nT. Based on these results, it can be seen that the anomalous value is low anomaly shaded in blue to green with anomaly values between -1771.8 nT to -306.2 nT. Moderate anomaly, coloured in yellow to orange has values between -306.2 nT to 268.3 nT. High level, red to pink has magnetic anomaly from 268.3 nT to 1089.9 nT. The tendency of negative magnetic intensity is thought to be caused by the presence of heat sources, reservoirs and the influence of demagnetized volcanic rocks. This negative magnetic intensity always occurs in geothermal

studies because ferromagnetic minerals present in rock layers will lose their magnetic properties when there is an increase in temperature (Telford et al., 1990).

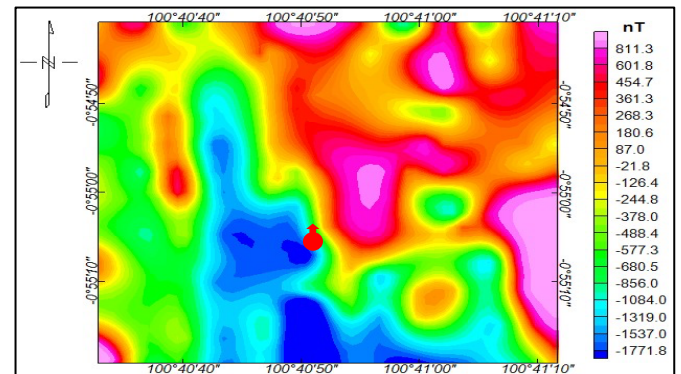


Figure 3. Magnetic anomaly contour map

The magnetic field anomaly obtained still has the influence of magnetic dipole-dipole pairs which are described in the form of positive magnetic value closures with negative magnetic value closures. Magnetic dipoles are anomalies originating from one object that is formed due to the influence of declination and inclination angles that change the direction of rock magnetization. To eliminate the influence of the magnetic dipole, it is necessary to perform reduction to pole (RTP) transformation.

Reduction to Pole (RTP)

Magnetic field anomaly data after RTP process is shown in Figure 4. Low magnetic anomaly is located in the northeast, center, and southeast part of the study area. Its position moves slightly to the north after reduction to pole. This movement is due to the research area being in the 47s UTM zone or at the geographical south latitude of the earth. The result of reduction to pole causes changes in the value of the magnetic anomaly range from -1730.4 to 1909.0 nT to -1258.1 to 1524.7 nT. There was a decrease in the range or data range from 3639.4 nT to 2782.8 nT because after reduction to the pole the dipole effect turns into a monopole and the dominance of the anomaly value becomes negative so that the anomaly will decrease.

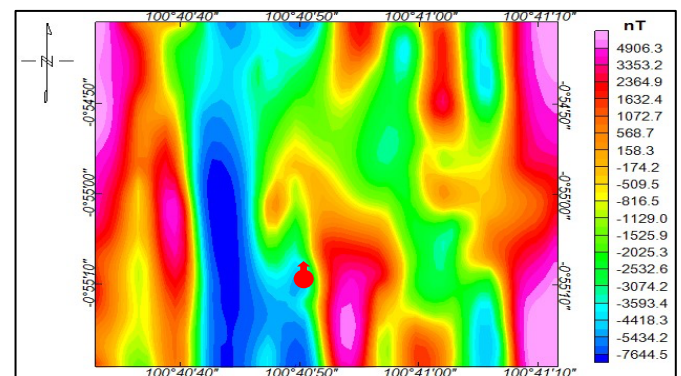


Figure 4. Reduction to pole contour map

Upward Continuation

The result of upward continuation on 50, 100 and 200 m distance is described on Figure 5(a), 5(b) and 5(c), respectively. On 50 m upward continuity contour map, the anomaly does not look different from the contour of the magnetic anomaly so that it does not show regional magnetic anomaly, but on the 100 m distance, upward continuity contour shows a regional magnetic anomaly to interpret, besides that the local effect has not been completely eliminated. It describes the rock composition in the study area. The results of 200 m upward continuation seem to be too dominant for regional effects and without the influence of local effects at shallow depths, so that the original anomalies on the contour map are no longer visible. Based on this analysis, the continuity contour map at height of 100 m was used for 2-dimensional modeling.

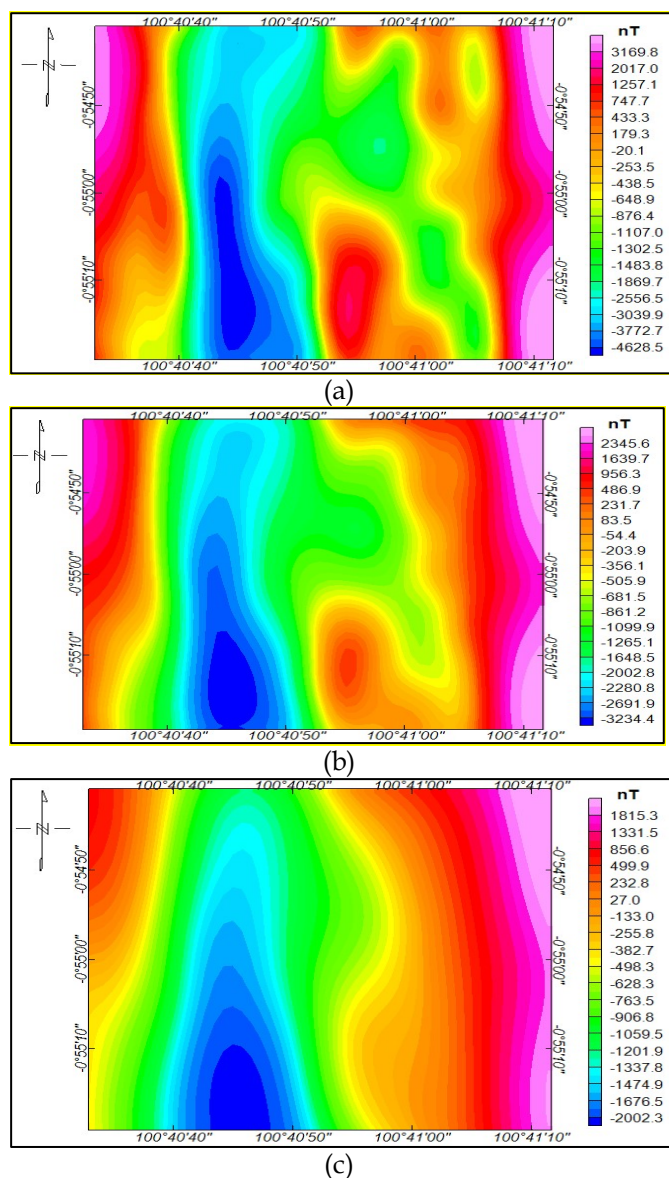


Figure 5. Upward continuation at (a) 50 m, (b) 100m and (c) 200 m

Two-Dimensional Modeling

On the upward continuation contour map with a height of 100 m, slice is made to describe the subsurface structure. The data from the incision is then used as input for modeling, in the form of topographic data and anomaly values. Slice A-A' was chosen because it intersects the positive contour pattern and the negative contour pattern with a path length of 1545 m. This incision passes through the fault zone indicated by the dotted line in Figure 6 which is supported by geological data. This fault zone plays a very important role in the process of geothermal fluid outflow through subsurface fractures. Another reason is that the A-A' incision also passes through the manifestation of the geothermal surface in the form of hot springs at a distance of about 675 m from the line.

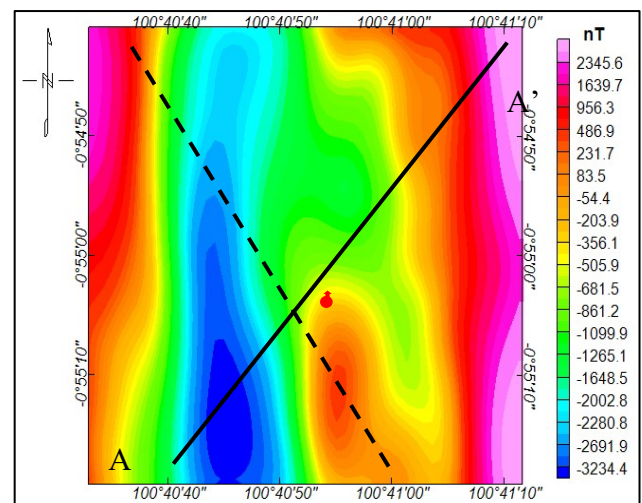


Figure 6. Slices on the contour map

In the A-A' slice, it passes through the negative contour pattern located in the northeast to the positive contour pattern in the northwest. The parameters used in this modeling are IGRF value of 42866,35 nT, declination angle of -0,1139 degrees, inclination angle of -19,02705 degrees, and maximum depth of 1000 m from ground level.

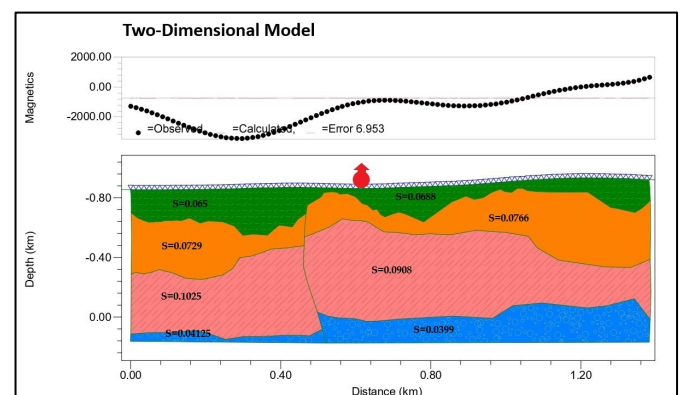


Figure 7. Subsurface 2D Model on A-A' slices

Table 1. Interpretation of the results of the A-A' slice modeling

Anomaly Geometry	Depth (m)	Susceptibility Value (SI)	Interpretation
Layer 1	200	0.0651-0.0688	Clay
Layer 2	200-400	0.0729-0.0766	Andesite, breccia, pyroclastic
Layer 3	300-950	0.0908-0.1025	Andesite, breccia, pyroclastic
Layer 4	850-1000	0.04	Andesite and pyroclastic

The modeling result in Figure 7 shows that there are 4 different layers. For the type of rock in each layer, it is necessary to add additional data in the form of geological data to reduce the high ambiguity (Corbel, S., Schilling, O., Horowitz, F.G., Reid L.B., Sheldon, H.A., Timms, N.E., Wilkes, 2012). Table 1 can be used to describe rock conditions in geothermal areas with rock susceptibility in SI units (10^{-6}). The parameters shown are susceptibility, depth, and geometry.

Based on this modeling, it can explain the existence of a fault on the left of the model results as a place for geothermal fluid outflow in the study area and forming a manifestation in the form of a hot spring pool at Bukik Gadang same as that obtained by Mawarni (2018) and Zakaria (2016). The shape of the fault formed from the overall modeling is a normal fault with varying depths. It can be seen in the modeling of the AA' trajectory. The geological structure is assumed to be a normal fault because the rock layers have subsidence faults. Furthermore, at a depth of 850 m below the surface there is a decrease in the susceptibility value compared to the rock in the layer above it. This can occur due to the influence of heat originating from a heat source which can remove the magnetic properties of the rock (demagnetization). Therefore, this layer can be interpreted as the Bukit Gadang geothermal reservoir layer.

Three-Dimensional Modeling

The results of the 3D modeling are shown in Figure 8. The 3D model already has a conformity with the 2D model and geological map. The susceptibility values obtained ranged from 0 to 0.24 (SI units). It can be seen that there is a high orange to red closure with a value range of 0.14 - 0.24 (SI Units) located in the east. Low shutters are light blue to blue with a value range of 0 - 0.06 in the west. Based on geological data the eastern part with high susceptibility values is in the Batino rock formation. The western part of the model results is in the Jantan rock formation with low susceptibility.

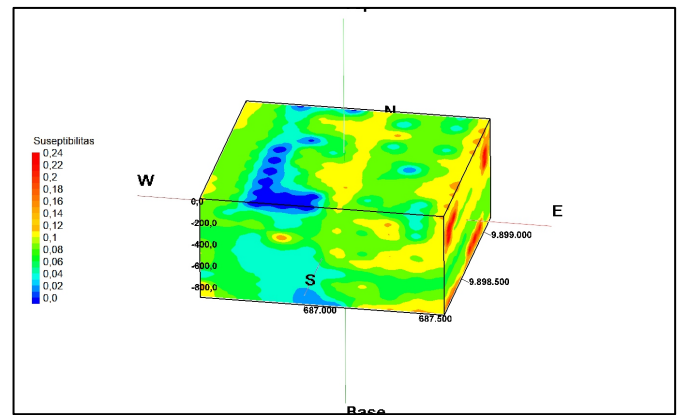


Figure 8. 3D model before reduction

Identification of fault lines can be determined based on the depth of rock around the fault line. If there is a difference in depth around the fault line, then the fault is an normal or thrust fault, whereas if there is no difference in rock depth, the fault is a shear fault (Heningtyas et al., 2020). Based on the modeling results, there are differences in the depth of the rocks around the fault line, thus strengthening the assumption that the fault line is a normal fault.

The position of the alleged fault line based on the modeling is in the northeast and parallel to the alleged fault line based on the geological map, extending from the southeast to the northwest as shown in Figure 9. The location of the alleged fault based on the modeling is shown by a dotted red line, while the fault on the geological map is shown by a black line. The fault segment extends from the southeast of the Batino Rock Formation and the Jantan Rock Formation with a direction of N160°E.

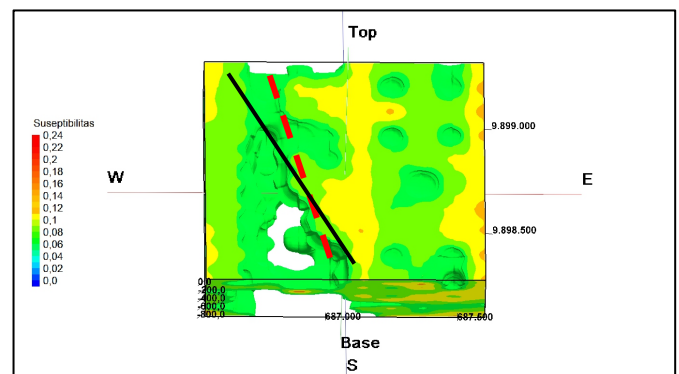


Figure 9. Presence of faults based on geological maps and 3D modeling

Figure 10 shows a difference in the height of Jantan rock formation. The height difference can be seen at a depth of 400-700 m and 100-200 m indicated by the black line that is identified as an alleged fault path based on modeling. at that depth there has been a decrease in one of the rock blocks which indicates the presence of a normal fault. This type of normal fault has also been

identified by previous studies such as Hanafy (2012) in eastern Qaret El Haddadin, Cairo city and Siler (2019) in Nevada and Oregon which is characterized by a downward movement of one of the rock blocks.

The fault structure at Bukik Gadang is estimated to be at a depth of 300-800 m or at the border of the Jantan and Batino Formation. This is indicated by the absence of differences in rock heights around the fault at a depth of less than 300 m in Figure 10. This fault line is also thought to be associated with the presence of hot springs from the Bukit Gadang as a place for geothermal fluid to flow from the reservoir rock layer to the surface. Normal faults can control geothermal fluid rise through the northwest-southeast trending fracture (James, 1987).

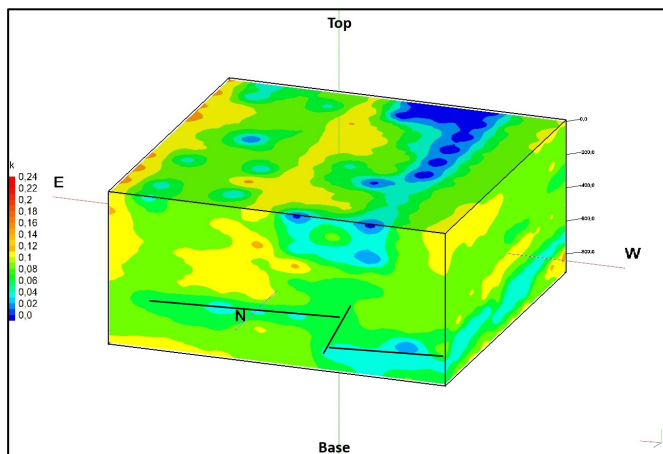


Figure 10. The difference in rock depth around the fault from the north from the modeling results

Conclusion

The results showed that the geological structure in the hot spring manifestation of Bukit Gadang is in the form of a normal fault with a relatively southeast-northwest direction. Magnetic data shows that there are differences in rock depths ranging from 100-200 meters. The fault begins to be seen at a depth of 300 m below the surface, getting lower and clearer to a depth of 800 m. The fault segment extends from the southeast of the Batino rock formation and the Jantan rock formation in the direction of N160°E. The existence of this fault serves as a place for geothermal fluid outflow. The distribution of magnetic field anomalies in the study area has a value ranging from -1771.8 nT to 1089.9 nT which is dominated by low anomalies. This is due to the presence of heat sources and demagnetization of subsurface rocks. The subsurface rock structure is dominated by pyroclastic flow units and andesitic lava rock from male volcanic formations and inner volcanic formations. In 2D modeling obtained a caprock layer on the top layer with an average depth of 850 meters below the surface. The reservoir rock layer is below the caprock layer which is characterized by demagnetization.

Acknowledgements

Authors are thankful to FMIPA Universitas Andalas for funding this research under contract No. 22/UN.16.03.D/PP/FMIPA/2021.

References

- Bukhari, S. K. (2019). Magnetic susceptibilities and fault surface anomalies. The study of land magnetic data & interpretations. *International Journal of Recent Technology and Engineering*, 7(6), 1053–1056.
- Corbel, S., Schilling, O., Horowitz, F.G., Reid L.B., Sheldon, H.A., Timms, N.E., Wilkes, P. (2012). Identification and Geothermal Influence of Faults in the Perth Metropolitan Area, Australia. *Proceedings, 37 Workshop on Geothermal Reservoir Eng*, 1–8.
- Dinas Pertambangan dan Energi Provinsi Sumatera Barat. (2017). *Booklet Potensi Panas Bumi Sumatera Barat*. [https://sumbarprov.go.id/images/dinasesdm/Booklet Potensi Panas Bumi Sumbar Englis.pdf](https://sumbarprov.go.id/images/dinasesdm/Booklet%20Potensi%20Panas%20Bumi%20Sumbar%20Englis.pdf)
- El All, E. A., Khalil, A., Rabeh, T., & Osman, S. (2015). Geophysical contribution to evaluate the subsurface structural setting using magnetic and geothermal data in El-Bahariya Oasis, Western Desert, Egypt. *NRIAG Journal of Astronomy and Geophysics*, 4(2), 236–248. <https://doi.org/10.1016/j.nrjag.2015.09.003>
- Fitrochaton Chasanah, A., Setyawan, A., & Dani Wardhana, D. (2018). Identifikasi struktur sesar daerah manifestasi panas bumi "X" di Kabupaten Manggarai Nusa Tenggara Timur berdasarkan analisis Horizontal Gradient. *Youngster Physics Journal*, 07(1), 11–18.
- Hanafy, S. M., Aboud, E., & Mesbah, H. S. A. (2012). Detection of subsurface faults with seismic and magnetic methods. *Arabian Journal of Geosciences*, 5(5), 1163–1172. <https://doi.org/10.1007/s12517-010-0255-6>
- Heningtyas, H., Wibowo, N. B., & Darmawan, D. (2020). Pemodelan 2D dan 3D Metode Geomagnet untuk Interpretasi Litologi dan Analisis Patahan di Jalur Sesar Oyo. *Jurnal Lingkungan Dan Bencana Geologi*, 10(3), 115–126. <https://doi.org/10.34126/jlbg.v10i3.157>
- Hidayat, R., & Putra, A. (2014). Penentuan Tipe Fluida Sumber Mata Air Panasdi Kecamatan Gunung Talang, Kabupaten Solok. *Jurnal Ilmu Fisika | Universitas Andalas*, 6(2), 74–80. <https://doi.org/10.25077/jif.6.2.74-80.2014>
- Idral, A. (2011). Effects of Subsurface Topography and Hydrogeology on Gunung Talang Hot Water Systems, Sumatra, Indonesia: an Analysis Based on. *Proceedings of 36th Workshop on Geothermal Reservoir Engineering*.

- James, E. D. (1987). Fault-dominated geothermal reservoirs. *AAPG (Am. Assoc. Pet. Geol.) Bull.;*(United States), 71(CONF-870606-).
- Kholid, M., & Marpaung, H. (2011). Survei Magnetotellurik Daerah Panas Bumi Bukit Kili-Gunung Talang, Kabupaten Solok, Sumatra Barat. *Prosiding Hasil Kegiatan Pusat Sumber Daya Geologi. Bandung, Indonesia: Geological Agency of Indonesia.*
- Maulidan, I. F., Tri Suci, R., Mahendra, A., & Putra, A. (2021). Interpretation of Subsurface Structure Based on the Magnetic Data at Semurup Geothermal Area Kerinci. *Jurnal Ilmu Fisika | Universitas Andalas*, 13(2), 101-108. <https://doi.org/10.25077/jif.13.2.101-108.2021>
- Mawarni, L., Maryanto, S., & Nadhir, A. (2018). Magnetic method used in geothermal reservoirs identification in Kasinan-Songgoriti, East Java, Indonesia. *Environmental and Earth Sciences Research Journal*, 5(4), 87-93. <https://doi.org/10.18280/eesrj.050402>
- Munandar, A., Suhanto, E., Kusnadi, D., Idral, A., & Solaviah, M. (2003). Penyelidikan Terpadu Daerah Panas Bumi Gunung Talang Kabupaten Solok-Sumatera Barat. *Kolokium Hasil Kegiatan Inventarisasi Sumber Daya Mineral. Bandung, Indonesia: Geological Agency of Indonesia.*
- Naryanto, H. S. (1997). Kegempaan di Daerah Sumatra. *Alami: Jurnal Teknologi Reduksi Risiko Bencana*, 2(3), 3-7.
- Qodri, R. R., & Putra, A. (2018). Studi Alterasi Hidrotermal dan Mineralisasi Batuan di Sekitar Mata Air Panas Garara Bukit Kili, Kabupaten Solok, Sumatera Barat. *Jurnal Fisika Unand*, 7(3), 246-252. <https://doi.org/10.25077/jfu.7.3.246-252.2018>
- Rohaendi, N., & Agustine, F. (2016). Geological and Mineralogical Studies on Long - Term Development of Geothermal Area : Case study of Fault Fracture Density Analysis of Remotely Sensed Lineaments of Gunung Talang Geoth ... Geological and Mineralogical Studies on Long - Term Development of. In *Pit Iagi* (Issue March). PIT IAGI Ke-45.
- Siler, D. L., Faulds, J. E., Hinz, N. H., Dering, G. M., Edwards, J. H., & Mayhew, B. (2019). Three-dimensional geologic mapping to assess geothermal potential: examples from Nevada and Oregon. *Geothermal Energy*, 7(1), 1-32. <https://doi.org/10.1186/s40517-018-0117-0>
- Sundhoru, H., Dwipa, S., Simanjuntak, J., & Nasution, A. (2001). Geothermal Fluids and Surface Manifestation in Gou Area, Flores Island: an Applied of Geoscientific Surveys. *Proceeding of the 5th INAGA Annual Scientific Conference and Exhibitions.*
- Taqiuddin, Z. M., Nordiana, M. M., & Rosli, S. (2017). The Identification of Seulimeum Fault System in Iejeu Aceh Besar (Indonesia) Using 2-D Resistivity Imaging Method. *IOP Conference Series: Earth and Environmental Science*, 62(1), 533-541. <https://doi.org/10.1088/1755-1315/62/1/012015>
- Telford, W. M., Geldart, L. P., & Sheriff, R. E. (1990). *Applied geophysics*. Cambridge university.
- Utami, Z. D., & Putra, A. (2018). Penentuan Karakteristik Fluida dan Estimasi Temperatur Reservoir Panas Bumi di Sekitar Gunung Talang. *Jurnal Fisika Unand*, 7(2), 130-137. <https://doi.org/10.25077/jfu.7.2.130-137.2018>